communications biology

A Nature Portfolio journal

Article

https://doi.org/10.1038/s42003-025-08183-9

Gasdermin-D pores induce an inactivating caspase-4 cleavage that limits IL-18 production in the intestinal epithelium

J. K. Bruce[1,2], L. Y. Li[1], Y. Tang[3], E. G. Forster[3], N. J. Winsor[1], P. Y. Bi[3], C. Krustev[3], S. Keely[2], J. E. Lee[3], J. R. Rohde[4], H. Y. Gaisano[5], D. J. Philpott[1] & S. E. Girardin[1,3] ✉

Intestinal epithelial-derived IL-18 is critical for homeostatic intestinal barrier function and is secreted through Gasdermin D (GSDMD) pores. Inflammasome activation is a prerequisite for both IL-18 maturation and GSDMD pore formation. However, GSDMD pores also cause pyroptotic cell death, which could be detrimental to the intestinal epithelial barrier. How epithelial cells balance the need to secrete IL-18 and to maintain barrier integrity remains poorly understood. In human intestinal epithelial cell lines and in primary human epithelial intestinal organoids, but not in immune cells, GSDMD plasma membrane pore formation by LPS electroporation and by gram-negative bacterial infection induced a non-conventional p37 caspase-4 fragment that was associated with reduced levels of mature IL-18. By contrast, limiting GSDMD plasma membrane pores pharmacologically and via point-mutagenesis prevented caspase-4 cleavage and increased IL-18 production, suggesting that p37 caspase-4 cleavage may regulate IL-18 maturation in the intestinal epithelium. In support, co-expression of caspase-4 cleavage mutants and IL-18 in HEK293T cells revealed that non-cleavable caspase-4 produced more mature IL-18 than cleaved caspase-4. Overall, these studies suggest that epithelial inflammasomes encode feedback pathways that control the balance between cytokine secretion and cell death. This may be an important mechanism to ensure homeostatic IL-18 production in the intestinal epithelium.

Inflammasomes are innate immune signalling complexes that recognise a diverse range of inflammatory molecules to activate inflammatory caspases[1]. Inflammatory caspase activation leads to cleavage of gasdermin-d (GSDMD)[2,3] and the cytokines IL-18 and IL-1β. Cleaved GSDMD forms pores in the plasma membrane that facilitate the release of biologically active IL-18 and IL-1β[4]. GSDMD pores also lead to the inflammatory cell death known as pyroptosis[5].

Inflammasomes are most widely studied in the context of myeloid cells where rapid lytic death of singular cells eliminates a pathogen's replicative niche. The pyroptotic cell carcass traps bacteria and the cell releases phagocytic chemo-attractants[6]. Thus, in myeloid cells, cellular lysis is an efficient mechanism to rapidly contain infections. Inflammasomes are also key defenders of epithelial barriers, where rapid lytic cell death of epithelial cells would be detrimental to tissue function. In mice, intestinal epithelial inflammasome activation results in the rapid GSDMD-dependent extrusion of infected epithelial cells[7,8]. Barrier integrity is maintained by caspase-dependent actin rearrangements that rapidly seal the space around the extruded cell[7]. Less is known about the effect of inflammasome activation in the human intestinal epithelium; however, caspase-4 appears to be the most critical effector of inflammasome activation and caspase-4, rather than caspase-1, restricts bacterial replication and facilitates IL-18 release[9,10].

While current research efforts have placed emphasis on understanding the role of epithelial cell death and expulsion, intestinal inflammasomes additionally activate and release IL-18. Epithelial-derived IL-18 protects the epithelium from inflammation and is involved in the expansion of epithelial stem cells[11]. Additionally, during infection, IL-18 recruits neutrophils and natural killer cells to restrict pathogen dissemination[12]. As described above, the current model states that when an epithelial inflammasome is activated, the affected cell is rapidly extruded into the intestinal lumen. If this is the only outcome of caspase-4 activation, it is difficult to reconcile how

[1]Department of Immunology, University of Toronto, Toronto, ON, Canada. [2]School of Biomedical Sciences & Pharmacy, University of Newcastle, Newcastle, NSW, Australia. [3]Department of Laboratory Medicine and Pathobiology, University of Toronto, Toronto, ON, Canada. [4]Department of Microbiology and Immunology Dalhousie University, Halifax, NS, Canada. [5]Department of Medicine and Physiology, University of Toronto, Toronto, ON, Canada.
✉e-mail: Stephen.girardin@utoronto.ca

caspase-4 can also produce and secrete IL-18 while maintaining a functional epithelial barrier.

Until recently, it was thought that cell death terminated inflammasome signalling and cytokine production. However, studies are increasingly showing that cells have mechanisms to modulate pyroptosis and prevent cell death following inflammasome activation. GSDMD pore-induced calcium influx induces the ESCRT system to remove pores from the plasma membrane to limit pyroptosis[13]. Certain cell types can secrete inflammasome-dependent IL-1β for up to 72 h while remaining viable[4,14,15]. These studies reveal that there is dynamic regulation in the induction of pyroptosis. It has been proposed that the balance of pyroptosis and cytokine release is controlled by the degree to which a cell can activate pore repair pathways[16]. However, this fails to account for a mechanism to turn-off inflammasome signalling, stop cytokine production and return to homoeostasis. The mechanisms that fine-tune pyroptosis are unclear, however they may be particularly important at epithelial barriers where minimising cell death while facilitating cytokine release is so important for maintaining barrier integrity and orchestrating a wider immune response.

In this study, we investigated how caspase-4 regulates IL-18 production in the human intestinal epithelium. We demonstrate that full length caspase-4 matures IL-18, and that caspase-4 cleavage is associated with reduced IL-18 levels, suggesting that caspase-4 cleavage may be a mechanism to limit rather than induce IL-18 production. We further show that GSDMD plasma membrane pore formation induces caspase-4 cleavage into a 37 kDa fragment. This fragment was not observed following caspase-4 activation in immune cells and was inconsistent with previously reported autocatalytic cleavage fragments, suggesting that GSDMD plasma membrane pore formation induces a factor that cleaves caspase-4 in intestinal epithelial cells. Under conditions of reduced GSDMD pore formation, we observed an absence of caspase-4 cleavage and increased IL-18 production. Together, these data suggest that GSDMD plasma membrane pore formation induces an inhibitory feedback mechanism to modulate caspase activity and control cytokine production. We propose that this may be an important factor in regulating the balance between pyroptosis and cytokine secretion in human intestinal epithelial cells. Overall, this work further characterises how caspase-4 functions in the human intestinal epithelium and defines a mechanism for regulation of human epithelial inflammasome signalling, and it explores how inflammasomes may be regulated to dynamically control the balance between cytokine secretion and cell death.

Results

Loss of GSDMD results in IL-18 hyperproduction in human epithelial cells

To activate the non-canonical inflammasome, we electroporated LPS into human epithelial HCT116 cells. LPS electroporation led to cell lysis (Fig. 1a), GSDMD cleavage (Fig. 1b) and IL-18 release (Fig. 1c) that was dependent on caspase-4 and GSDMD expression. Unexpectedly, when examining IL-18 production by western blot, we observed high levels of mature IL-18 in the lysates of GSDMD$^{-/-}$ cells (Fig. 1d). Mature IL-18 is secreted through GSDMD pores; therefore, to compare the total amount of IL-18 produced, we lysed cells into the supernatant and measured IL-18 (hereafter referred to as total IL-18) via ELISA. Surprisingly, we observed that GSDMD$^{-/-}$ cells produced approximately 10 times more mature IL-18 than WT cells (Fig. 1e). This increase in IL-18 production could not be accounted for by elevated expression of pro-IL-18, (Fig. 1f), nor could it be inhibited by blocking transcription (Fig. 1g, Supplementary Fig. 1a) or translation of the pro IL-18 substrate (Fig. 1h, Supplementary Fig. 1b). Thus, GSDMD limits IL-18 maturation following caspase-4 activation in human HCT116 intestinal epithelial cells.

To confirm that our phenotype was not due to off target effects following CRISPR cas9 genome editing, or a result of mutations in cancer cell lines, we knocked down GSDMD in primary human intestinal epithelial organoids and in C2bbe1 cells using RNA interference (RNAi) techniques (Fig. 2a–f). In both cases, GSDMD knockdown reduced LPS-induced cell lysis (Fig. 2b, e) and increased IL-18 maturation (Fig. 2c, f). To determine if our findings were also observed in hematopoietic cells, we knocked GSDMD down in human THP1 monocytes (Fig. 2g–i). Knocking down GSDMD significantly reduced LPS-electroporation-induced LDH release (Fig. 2h) and slightly increased IL-18 production (Fig. 2i), however the degree to which silencing GSDMD affected IL-18 production in human monocytes was minimal compared to that observed in intestinal epithelial cells (Fig. 2c, f compared to Fig. 2i). Based on these results, we concluded that GSDMD regulates IL-18 maturation in a tissue specific fashion and has a particularly large impact upon IL-18 maturation in human intestinal epithelial cells.

Epithelial cell IL-18 hyperproduction occurs in the absence of LPS-induced caspase cleavage

It is widely reported that oligomerization-induced autoproteolysis is generally required for caspase activation[17]. Indeed, measuring the production of caspase-1 p20 is the gold standard for assessing caspase-1 activation, and increased cleavage is thought to reflect a greater degree of caspase activation. Caspase-4 was reported to be cleaved into p31 and p33 fragments[18], and caspase-4, rather than caspase-1, is required for IL-18 production in human intestinal epithelial cells[9,10,19] (Supplementary Fig. 1c-e). We therefore hypothesized that increased caspase-4 cleavage led to increased IL-18 production in GSDMD-deficient cells and attempted to measure this by western blot. LPS electroporation resulted in a reduction of pro-caspase-4 levels in the lysate of WT epithelial cells, and the appearance of cleavage fragments in the supernatant (Fig. 3a, b; lanes 1 and 2). Interestingly, in both HCT116 cells (Fig. 3a) and primary human intestinal epithelial cells (Fig. 3b) we observed cleavage fragments of approximately 37 kDa, not the anticipated 33 kDa or 31 kDa. Importantly, we observed no evidence of LPS-induced caspase-4 cleavage in *GSDMD*$^{-/-}$ HCT116 or GSDMD KD primary epithelial cells (Fig. 3a, b). Therefore, in GSDMD-deficient intestinal epithelial cells, increased IL-18 production occurs in the absence of caspase-4 cleavage. Given this surprising result, we examined caspase-4 in THP1 immune cells. We observed a caspase-4 p31 fragment in lysates of both WT and GSDMD-knockdown THP1 cells following LPS electroporation (Fig. 3c). Therefore, contrary to epithelial cells, in immune cells GSDMD is not required for caspase-4 cleavage and GSDMD does not regulate IL-18 maturation. Interestingly, in THP1 cells, the generation of caspase-4 p31 was blocked by pre-treatment with the NLRP3 inhibitor MCC950 (Fig. 3d), suggesting that p31 fragment generation may be the secondary result of NLRP3 activation occurring downstream of GSDMD plasma membrane pore formation, rather than caspase-4 autoproteolytic activity. Of note, intestinal epithelial cells lack NLRP3 expression (Supplementary Fig. 1f) and do not respond to typical NLRP3 agonists such as nigericin (Supplementary Fig. 1g). Given that LPS did not induce caspase-4 processing in GSDMD-deficient epithelial cells, we considered that loss of GSDMD might induce caspase-4-independent IL-18 production. Caspase-1 expression was very low in intestinal epithelial cells (Fig. 3e, Supplementary Fig. 1c), and in contrast to THP1 cells, we observed no caspase-1 cleavage following LPS electroporation in HCT116 epithelial cells (Fig. 3e). Similarly to caspase-4, LPS electroporation induced caspase-5 processing in WT but not *GSDMD*$^{-/-}$ HCT116 epithelial cells (Fig. 3f). Thus, in epithelial cells, GSDMD is required for caspase-4 and caspase-5 cleavage and increased IL-18 production occurs in the absence of inflammatory caspase cleavage.

Caspase-4 cleavage is associated with decreased IL-18 production in intestinal epithelial cells

Given that we did not observe inflammatory caspase processing in *GSDMD*$^{-/-}$ cells, we wondered whether IL-18 processing was dependent on caspase activity, or if an alternative pathway was engaged. To test this hypothesis, we pre-treated cells with the pan-caspase inhibitor Z-VAD-FMK for 1 h prior to electroporation to block the activity of all caspases. Z-VAD-FMK treatment completely inhibited LPS induced cell lysis (Fig. 4a), IL-18 release (Fig. 4b) and blocked IL-18 maturation in both WT cells and

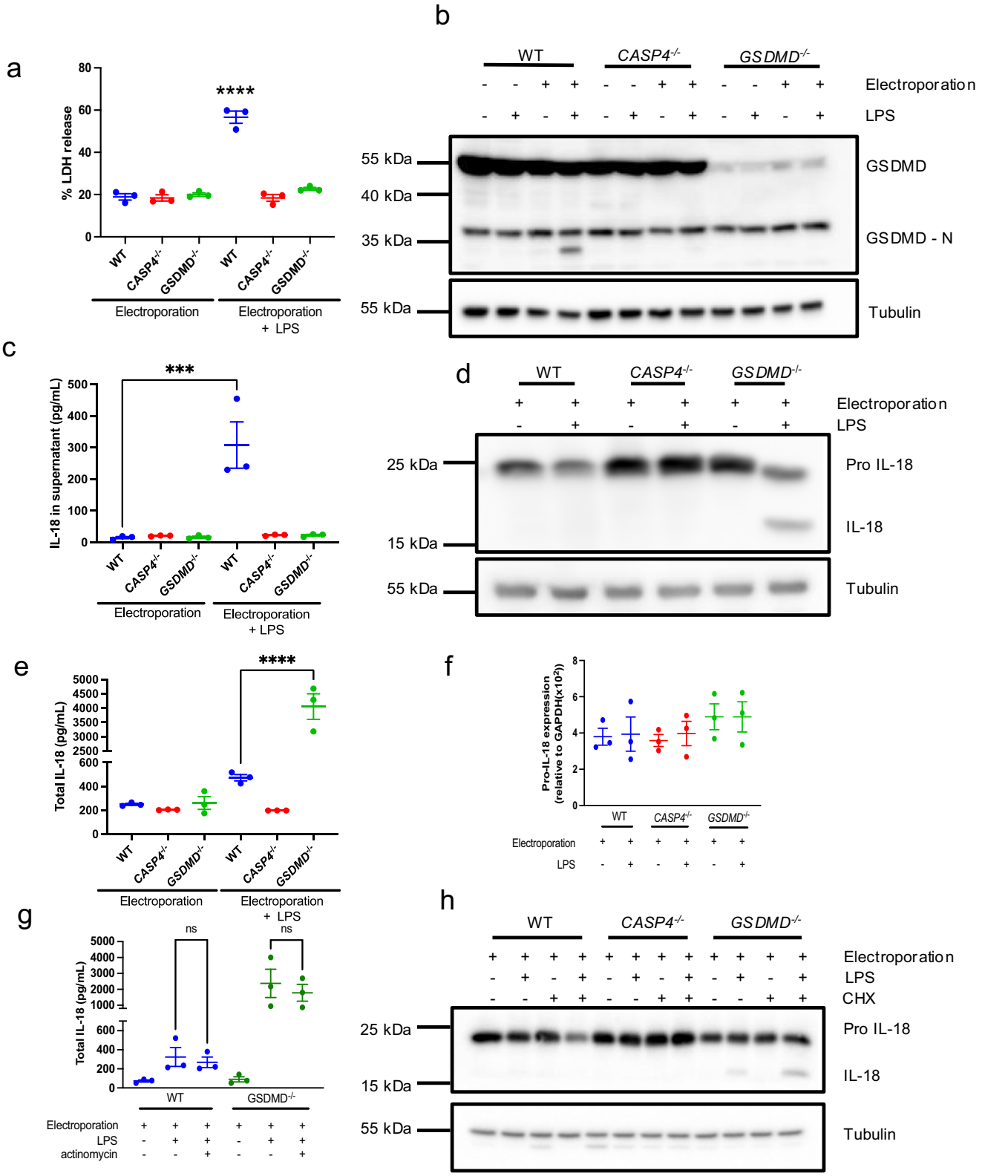

Fig. 1 | GSDMD limits IL-18 maturation in human intestinal epithelial cells. HCT116 human epithelial cells were electroporated with 2 μg LPS as indicated. Cells were harvested 3 h post electroporation. Cell lysis (**a**) was measured using LDH cytotoxicity assay. GSDMD (**b**) and IL-18 cleavage (**d**) were measured by western blot of whole cell lysates. IL-18 secretion was measured by ELISA in cell free supernatant (**c**). Total IL-18 (**e**, **g**) was measured by lysing cells into supernatant then conducting ELISA. Pro-IL-18 transcript levels were measured by qPCR (**f**). To block transcription, cells were pre-treated with actinomycin for 1 h prior to electroporation (**g**). To block translation, cells were incubated with cycloheximide (CHX) for 6 h prior to electroporation (**h**). Representative of at least 3 experiments, data displayed as mean ± S.E.M. $^{***}p < 0.005$, $^{***}p < 0.001$.

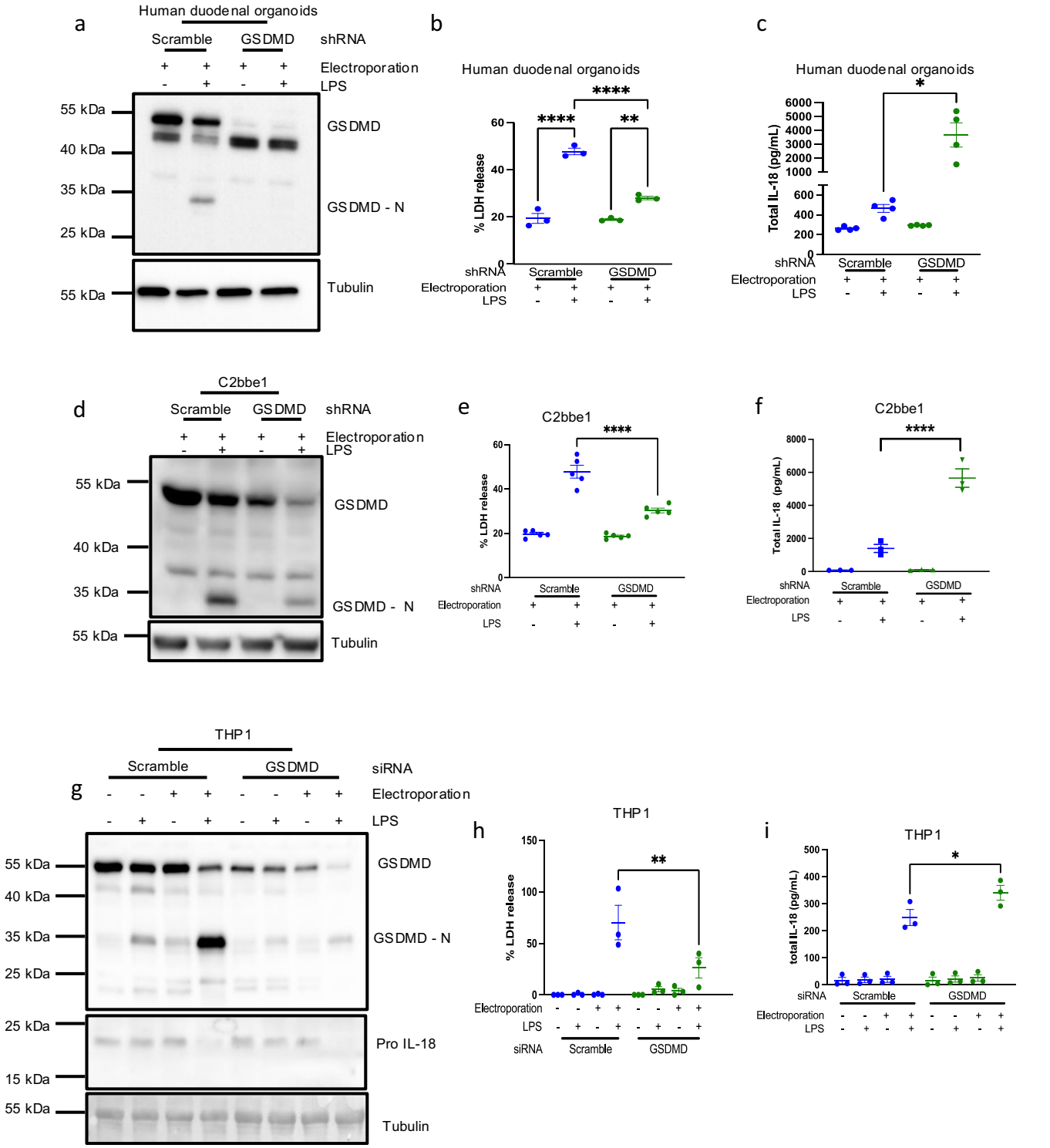

Fig. 2 | Overproduction of IL-18 is enhanced in intestinal epithelial cells. Human duodenal organoids (**a**–**c**), C2bbe1 intestinal epithelial cells (**d**–**f**) and THP1 human monocytes (**g**–**i**) were electroporated with 2 μg LPS as indicated. Cell lysis was measured by LDH assay (**b**, **e**, **h**), GSDMD expression and cleavage was measured by western blot (**a**, **d**, **h**), total IL-18 was measured by lysing cells into supernatant then conducting ELISA (**c**, **f**, **i**). Representative of at least 3 experiments, data displayed as mean ± S.E.M. $^{****}p < 0.001$, $^{**}p < 0.01$, $^{*}p < 0.05$.

GSDMD$^{-/-}$ cells (Fig. 4c), confirming that caspase catalytic activity is required for IL-18 processing in *GSDMD*$^{-/-}$ cells even in the absence of LPS-inducible caspase-1, 4 or 5 cleavages.

To further elucidate which caspase processes IL-18 in *GSDMD*$^{-/-}$ cells, we used RNAi techniques to knock down inflammatory caspases in GSDMD-deficient cells (Fig. 4d–f and Supplementary Fig. 1h–j). Knocking down caspase-4 (Fig. 4d) but not caspase-5 (Fig. 4e) or caspase-1 (Fig. 4f) blocked IL-18 production in both WT and GSDMD-deficient cells, confirming that caspase-4 and no other inflammatory caspases were required for IL-18 processing. However, it is important to note that caspase-4 functions as both the sensing protein and the executioner protein, and as such caspase-4 KD cells are unable to respond to intracellular LPS. To

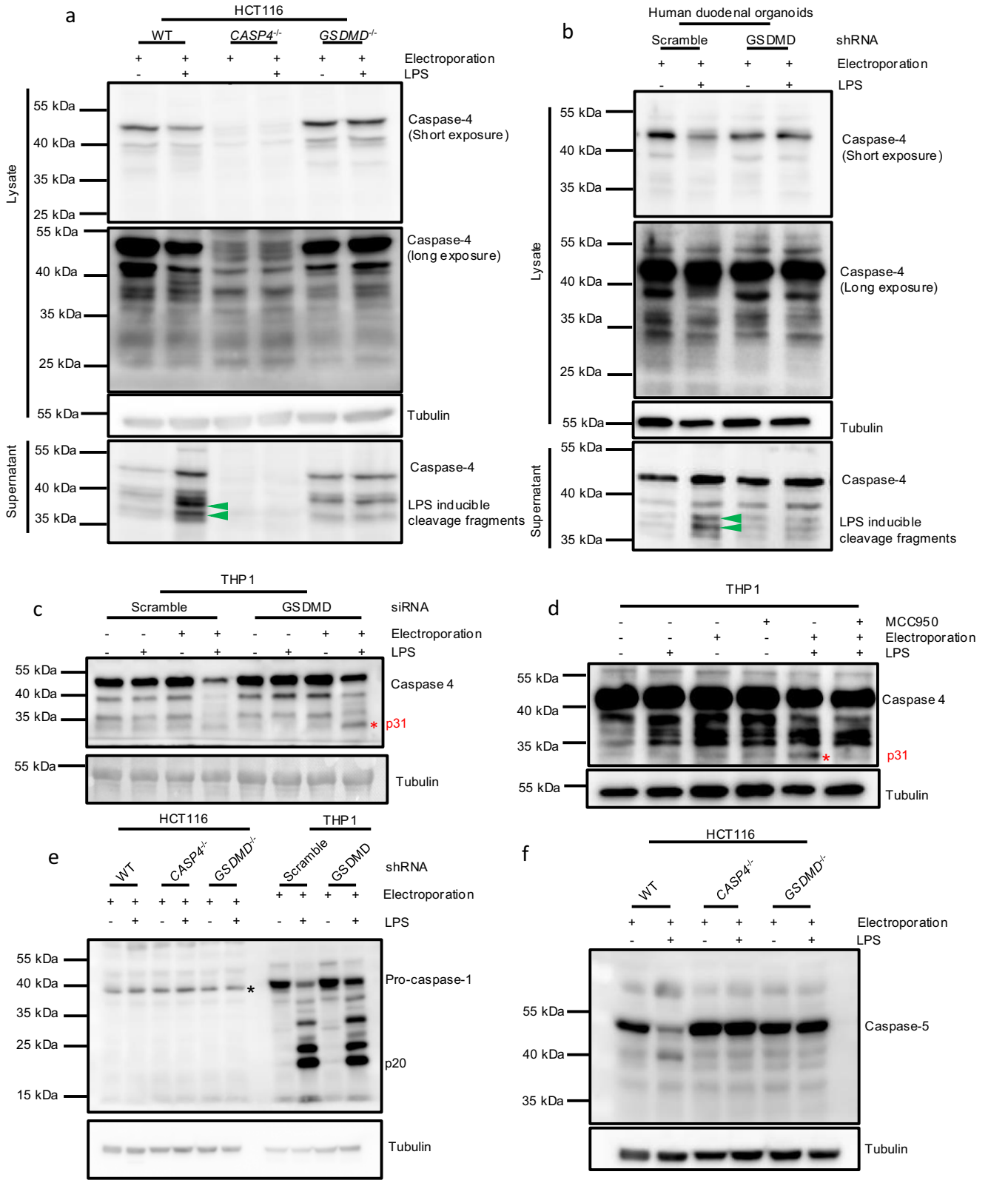

Fig. 3 | Blunted LPS-induced caspase-4 processing correlates with IL-18 hyper-production in GSDMD$^{-/-}$ epithelial cells. HCT116 epithelial cells (**a**, **e**, **f**), Human duodenal organoids (**b**) or human THP1 monocytes (**c**, **d**) were electroporated with 2 µg LPS. For (**d**) THP1 cells were co-treated with NLRP3 inhibitor MCC950. Inflammatory caspase activation was measured by western blot on whole cells lysates and supernatant where indicated. For (**e**) star indicates non-specific band. See Supplementary Fig. 1 for further explanation. Representative of at least 3 experiments.

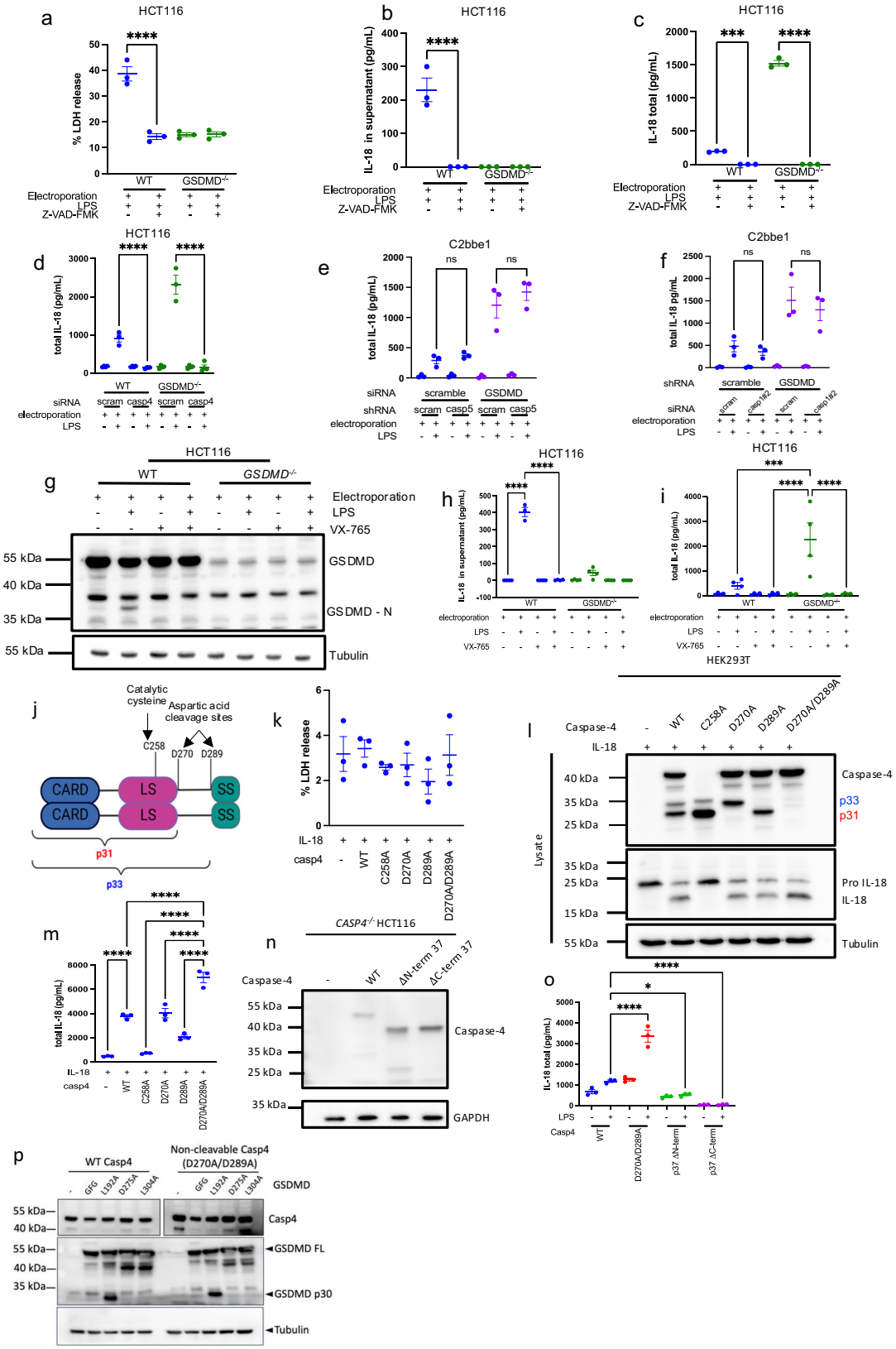

Fig. 4 | Non-cleaved caspase-4 matures IL-18 in human intestinal epithelial cells. HCT116 epithelial cells were treated with 2 μM of pan-caspase inhibitor Z-VAD-FMK (**a**–**c**), siRNA targeting caspase-4 (**d**) or with caspase-1/4 specific inhibitor VX-765 (**g**–**i**). C2bbe1 epithelial cells were transduced with shRNA or transfected with siRNA as indicated to generate double -caspase-1 or -5 and GSDMD knockdowns (**e**, **f**). For inflammasome activation, cells were electroporated with 2 μg LPS. HEK293T cells (**k**–**m**) or *CASP4*$^{-/-}$ HCT116 cells were transfected with caspase-4 expression vectors indicated in (**j**). HEK293T cells were harvested 16 h post transfection (**k**–**m**, **p**). HCT116 cells were electroporated with LPS 16 h post transfection (**n**, **o**). Cell lysis was measured by LDH cytotoxicity assay (**a**, **k**). Western blots were conducted on whole protein lysates (**g**, **l**, **n**, **p**). IL-18 release was measured by ELISA on supernatant alone (**b**, **h**) or by lysing cells into supernatant prior to ELISA (**c**, **d**, **e**, **f**, **i**, **m**, **o**). Representative of at least 3 experiments except for panel (**p**) ($N = 1$), data displayed as mean ± S.E.M. $^{****}p < 0.001$, $^{***}p < 0.005$.

address this issue, we pre-treated cells with the caspase-1/4 catalytic inhibitor VX-765 (Fig. 4g–i). In this model, cells can bind LPS via the unaffected CARD domain, but caspase-4 is rendered catalytically dead by modification of the catalytic cysteine[20]. Pre-treatment with VX-765 completely blocked GSDMD cleavage (Fig. 4g), IL-18 secretion (Fig. 4h) and IL-18 maturation (Fig. 4i), confirming that caspase-4 catalytic activity is required for IL-18 processing in both WT and GSDMD-deficient human intestinal epithelial cells.

Since our data indicated that full length caspase-4 is active against IL-18 and that cleavage is associated with reduced IL-18 maturation, we reasoned that full length caspase-4 was likely the species that cleaves IL-18 and postulated that GSDMD-facilitated cleavage might limit activity against IL-18. To test this, we generated caspase-4 expression vectors, mutated the known cleavage (D270 and D289) and catalytic (C258) sites[18] (as shown in Fig. 4j) and transiently overexpressed these together with IL-18 in HEK293T cells (Fig. 4k–m). In this system, overexpression facilitates caspase oligomerization and activation and as HEK293T cells do not express endogenous GSDMD, activation of caspase-4 does not lead to cell death (Fig. 4k) or plasma membrane pore formation (See Fig. 6i). As expected, caspase-4 was required for IL-18 processing, and mutation of the catalytic cysteine C258 prevented IL-18 cleavage (Fig. 4l, m). Interestingly, overexpression of catalytically dead (C258A) caspase-4 resulted in a band at approximately the same molecular weight as a reported autocatalytic product p31 (lane 3 Fig. 4l), suggesting that the cleavage at D270 is not the result of caspase-4 catalytic activity and that p31 is not active against IL-18. Mutation of individual autocleavage sites resulted in roughly equal amount of cleaved IL-18 as WT caspase-4 (Fig. 4l, m); however, mutation of both sites greatly increased IL-18 processing (Fig. 4l, m), demonstrating that the uncleavable full length caspase-4 is the form that produces the highest levels of mature IL-18. Similarly, in *CASP4*$^{-/-}$ HCT116 cells, cleavage-resistant caspase-4 generated more IL-18 following LPS activation (Fig. 4o) and retained the capacity to cleave GSDMD (Fig. 4p). To investigate the activity of our putative p37 fragment, we generated two constructs that approximately recapitulate the two possible cleavage fragments by removing 6 kDa from either the N-terminus or the C-terminus, and expressed these constructs in *CASP4*$^{-/-}$ HCT116 cells (Fig. 4n, o). Both p37 fragments generated less IL-18 than either the WT or the cleavage resistant caspase-4. However, this proxy approach has some limitations, since we were not able to determine exactly where the cleavage occurs to generate the p37 fragment, and future studies should aim at providing more definitive proof of the lack of activity of the naturally occurring p37 Casp4 fragment, once the exact cleavage site is identified.

GSDMD plasma membrane pore formation facilitates caspase-4 cleavage to limit IL-18 processing

We next sought to determine which function of GSDMD regulates IL-18 production and caspase-4 cleavage. We reasoned that cell lysis, GSDMD pore formation, or an effect of GSDMD cleavage on caspase-4 could each impact IL-18 processing. We first tested the effect of inhibiting cell lysis by pre-treating cells with glycine[21]. Glycine reduced cell lysis (Fig. 5a) but had no effect on GSDMD cleavage (Fig. 5b). Secreted IL-18 was equivalent between glycine and non-glycine treated cells, confirming that pore formation was intact (Fig. 5c). Importantly, glycine had no effect on total IL-18 production (Fig. 5d). Interestingly, in glycine-treated cells, p37 cleaved caspase-4 was detected in cell lysates (Fig. 5e), demonstrating that secretion of cleaved caspase-4 during cellular lysis does not limit IL-18 production. To further validate these results, we generated NINJ1 KD cells (Fig. 5f). As expected, NINJ1 KD reduced LDH release (Fig. 5g). Total IL-18 levels were equivalent between scramble and NINJ1 KD cells (Fig. 5h). Like glycine pre-treatment, NINJ1 KD did not prevent caspase-4 cleavage, but did prevent the release of a p37 caspase-4 cleavage fragment into cell supernatants (Fig. 5i). Together these findings demonstrate that cell lysis does not regulate p37 caspase-4 cleavage and IL-18 production.

We next sought to determine if GSDMD pore formation regulates IL-18 processing and caspase-4 cleavage into the p37 form. To assess this, we pretreated cells with dimethylfumerate (DMF). DMF has been reported to succinate cysteine residues, particularly C191, to prevent GSDMD N-terminal insertion into the plasma membrane[22]. Recent studies have shown that palmitoylation at C191 is critical for insertion of GSDMD-N into the plasma membrane[23,24]. DMF completely inhibited LPS-dependent cell lysis (Fig. 6a) but had no effect on GSDMD cleavage (Fig. 6b). DMF also prevented IL-18 release into the supernatant (Fig. 6c). Together these results indicate that DMF blocks plasma membrane pore formation, even in the presence of a GSDMD-N fragment. Importantly, blocking GSDMD plasma membrane pore formation limited caspase-4 cleavage (Fig. 6d) and increased total IL-18 levels (Fig. 6e). Altogether, our findings suggest that GSDMD plasma membrane pore formation induces caspase-4 cleavage to limit IL-18 processing.

Plasma membrane pore formation, not cell death, limits IL-18 production

We considered how cell death might impact IL-18 production and whether IL-18 production ceased because cells died. Indeed, in DMF-treated cells, a lack of plasma membrane pores could indicate cells survive longer, allowing more time for IL-18 production. Cell death likely impacts IL-18 production to a degree, however our data indicated additional mechanisms regulate caspase-4 cleavage independently of cell death.

Recent papers support the idea that GSDMD-N terminus damages mitochondria[24–26] and lysosomes[26] prior to plasma membrane pore formation. It is likely that this compromises cellular viability prior to plasma membrane pore formation[25]. Considering this, it is likely that pyroptosis is a multifactorial process, and that damage to intracellular organelles including mitochondria and lysosomes contributes to cell death prior to plasma membrane pore formation. To assess whether cell death limits IL-18 maturation, we assessed the kinetics of cellular viability and IL-18 production in DMF-treated cells (Fig. 6f, g). LPS electroporation reduced cellular viability to about 50% within 5 min of electroporation regardless of plasma membrane pore formation (i.e in both DMF and non-DMF treated conditions; Fig. 6f). From 1 to 3 h post electroporation, there was no further reduction in cellular viability. This is in line with other studies showing that inflammasome activation compromises mitochondrial integrity within 7.5 min[25] and that plasma membrane pore-independent processes alter cellular viability[25]. Importantly DMF-treated cells continued to produce IL-18 over the entire three hours of stimulation (Fig. 6g), indicating that IL-18 production is unaffected by reductions in cell viability.

To further test whether plasma membrane pore formation or cell death regulated IL-18 production, we transfected caspase-4 along with IL-18 and WT GSDMD or GSDMD with mutations that: (1) contains an N-terminal that does not form plasma membrane pores[27] (W48G and W50G—named GFG); (2) forms plasma membrane pores with less efficiency than WT GSDMD[28–30] (L192A); (3) cannot be cleaved (D275A); or (4) contain mutations in the exosite required for recognition by caspase-4[18] (L304A/L308A) into HEK293T cells. A schematic of the effect of each mutation is provided (Fig. 6h). We validated that each mutant had the intended effect on pore formation by monitoring propidium iodide (PI) uptake following transfection (Fig. 6i). Importantly, only WT GSDMD and L192A GSDMD formed plasma membrane pores (Fig. 6i). We measured cellular viability in our reconstitution system (Fig. 6j). Although GSDMD-GFG did not generate plasma membrane pores (Fig. 6i), it reduced cellular viability to the same extent as WT GSDMD (Fig. 6j). On the other hand, GSDMD L192A did not reduce cellular viability (Fig. 6j). Thus, GSDMD L192A forms plasma membrane pores but does not diminish cellular viability while GSDMD GFG does not form plasma membrane pores but does impact cellular viability. Importantly, when we compared IL-18 production between these two conditions, we observed that cells transfected with GSDMD GFG produced more IL-18 than cells transfected with GSDMD L192A (Fig. 6k, l), strongly suggesting that GSDMD pore formation and not cellular viability controls IL-18 production. Thus, in two independent models, plasma membrane pore formation, and not cell death, limits IL-18 production.

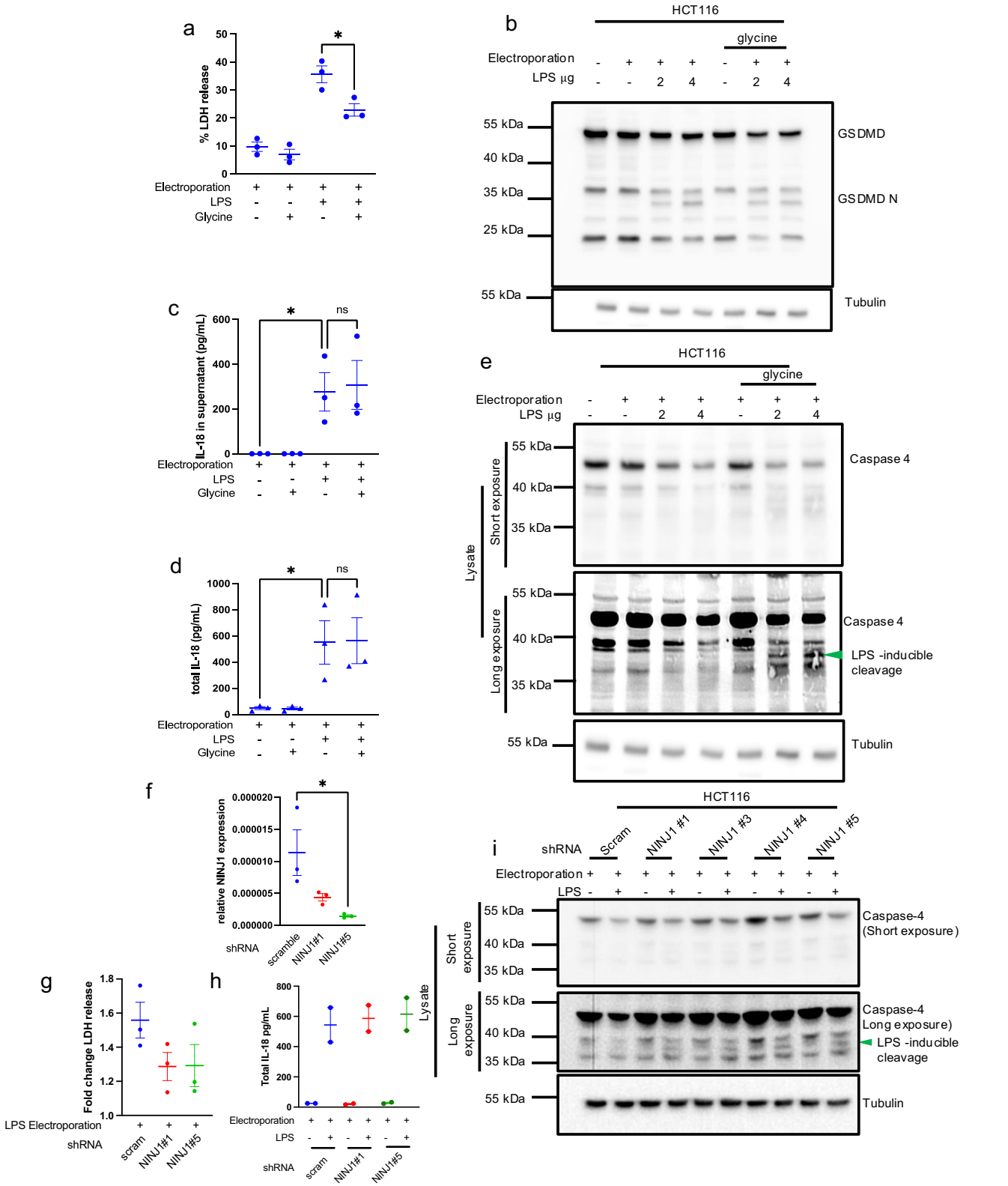

Fig. 5 | Cell lysis does not regulate caspase-4 cleavage and IL-18 production. **a**–**e** HCT116 cells were electroporated then placed in media with 10 mM glycine to prevent cell lysis. In panels (**f**–**i**), HCT116 cells were silenced for *NINJ1* expression using shRNA constructs, as indicated, before LPS electroporation. Cell lysis was measured by LDH cytotoxicity assay (**a**, **g**). GSDMD (**b**) and caspase-4 (**e**, **i**) cleavage was measured by western blots of whole cell lysates. IL-18 was measured by ELISA on supernatants (**c**), or on cells lysed into supernatant (**d**, **h**). The effect of *NINJ1* shRNA constructs 1 and 5 on NINJ1 expression in HCT116 cells was determined by qRT-PCR (**f**). Green arrow indicates LPS dependent caspase-4 cleavage products. Representative of at least 3 experiments (except for (**h**) where $n = 2$), data displayed as mean ± S.E.M. $^*p < 0.05$.

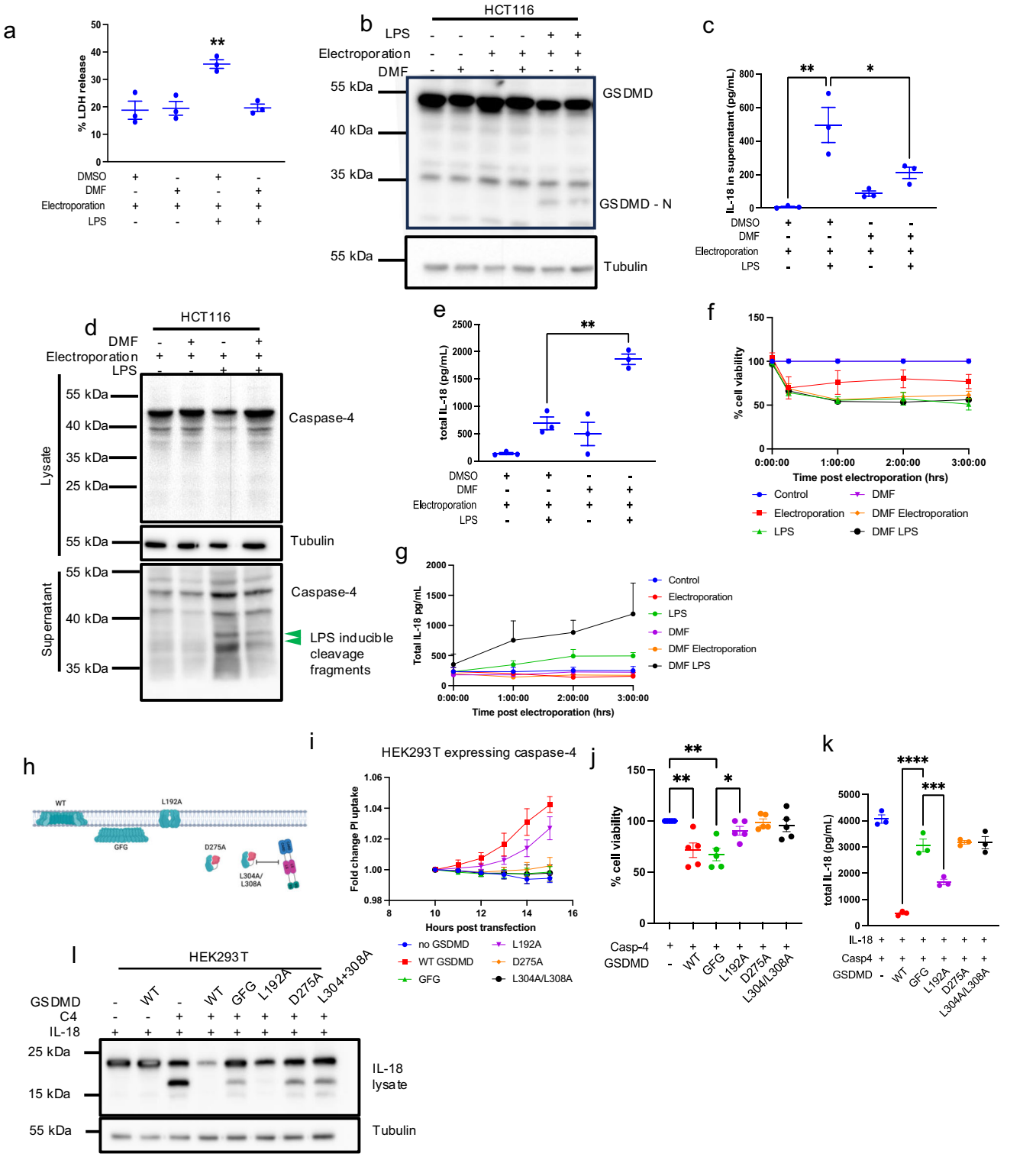

Fig. 6 | Blocking GSDMD pore formation inhibits caspase-4 cleavage and increases IL-18 production but does not prevent cell death. a–g HCT116 cells were pre-treated with 50 μM dimethylfumerate (DMF) for 1 h then electroporated with LPS and placed back into media containing 50 μM DMF. **h–l** GSDMD and mutants indicated in schematic (**h**) were generated. GFG contains point mutations at W48 and W50, that prevent insertion of pores into the plasma membrane. L192A is cleaved and forms pores with less efficiency that WT GSDMD, D275A cannot be cleaved, L304A/L308A cannot bind the caspase-4 exosite. Mutants were transiently transfected into HEK293T cells along with WT caspase-4 and IL-18. Cell lysis was measured by LDH (**a**), GSDMD, caspase-4 or IL-18 cleavage was measured by western blots on whole cell lysates or supernatant as indicated (**b**, **e**). IL-18 was measured by ELISA on supernatant alone (**c**), or on cells lysed into supernatant (**e**, **g**, **k**). Cellular viability was measured by CellTitre-Glo assay® at indicated timepoints for (**f**) or 16 h following transfection for (**j**). PI uptake was measured by calculating the mean fluorescence intensity (MFI) of each condition compared to non-transfected control (**i**). Representative of at least 3 experiments, data displayed as mean ± S.E.M. $^{****}p < 0.001$ $^{***}p < 0.005$, $^{**}p < 0.01$, $^{*}p < 0.05$. Panel (**h**) was created with Biorender.

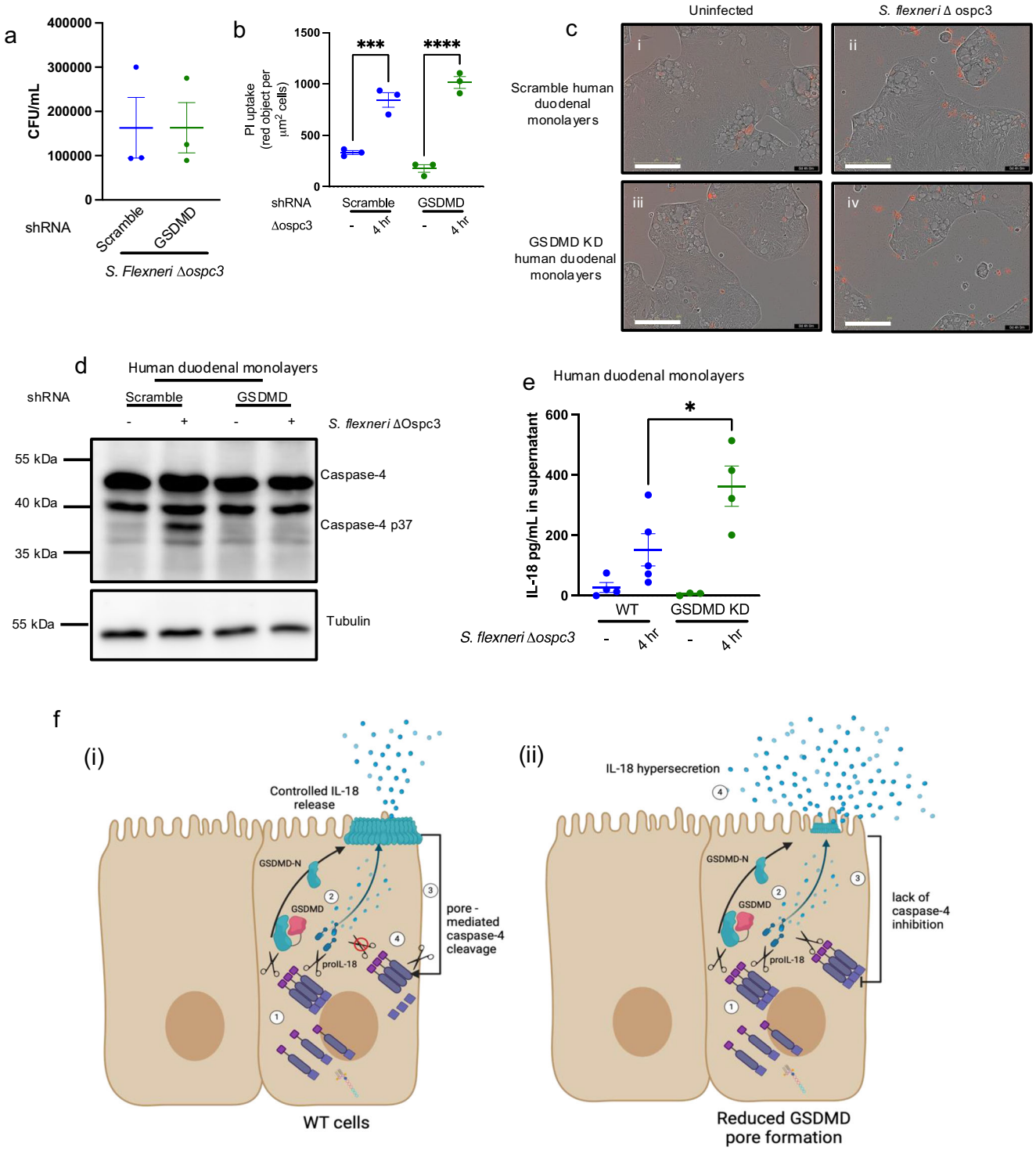

Fig. 7 | GSDMD regulates IL-18 production and caspase-4 cleavage during *Shigella* infection in primary human monolayers. Human duodenal organoids were trypsinised into single cells and seeded onto culture plates pre-coated with 1:40 Matrigel:PBS. Cells were infected with *S. flexneri* Δ ospc3 at an MOI of 100 for 4 h. CFUs in infected cells were enumerated (**a**), PI uptake was monitored using incucyte live cell imager and PI uptake was normalised per area confluency (**b**), images of monolayers taken 4 h post infection taken at 20x (i) scramble, uninfected; (ii) scramble, *Shigella flexneri* Δ ospc3, (iii) GSDMD KD uninfected, (iv) GSDMD KD *Shigella flexneri* Δ ospc3. Scale bars (indicting 200 micrometres) are depicted for each micrograph (**c**). Caspase-4 was measured in western blot of whole cell lysates (**d**), IL-18 secretion into the supernatant was measured by ELISA on cell free supernatants (**e**). A schematic of caspase-4 regulation (**f**). In (**f**) (i) LPS-induced caspase-4 activation (1) leads to activation of GSDMD and IL-18 (2). GSDMD pores lead to caspase-4 cleavage (3) and this stops IL-18 processing (4). In (**f**)(ii), during conditions of reduced GSDMD –mediated plasma pore formation, caspase-4 activation (1) leads to IL-18 processing. A lack of efficient pore formation reduces inhibitory feedback on caspase-4 (3). This leads to continued activity of caspase-4 on IL-18 and IL-18 hypersecretion (4). All experiments are representative of at least 3 experiments. Data displayed as mean ± S.E.M. $*p < 0.05$, $****p < 0.001$. Panel (**f**) created with Biorender.

Collectively our data suggests that plasma membrane pore formation induces caspase-4 cleavage to limit IL-18 processing. We attempted to investigate how plasma membrane pore formation induces caspase-4 cleavage. We investigated the impact of blocking autophagy[31], cathepsins[32,33], radical oxygen species[34] (ROS), calcium flux and the proteosome[35] on IL-18 maturation in our system. The results of these studies are presented in Supplementary Fig. 2a–i. None of these processes significantly impacted IL-18 production. Endoplasmic reticulum (ER) stress has been shown to induce caspase-4 cleavage[36], and we confirmed that thapsigargin treatment induced a p37 caspase-4 cleavage product (Supplementary Fig. 2j). We hypothesised that GSDMD pore formation may induce ER stress leading to caspase-4 cleavage. We therefore investigated if LPS electroporation induced ER stress by measuring XBP1 splicing[37] (Supplementary Fig. 2k) but did not observe ER stress using this proxy. Our hypothesis remains that GSDMD plasma membrane pore formation induces an undefined protease to cleave caspase-4. The identification of this protease and the nature of the physiological cues that would trigger this protease downstream of plasma membrane pore formation will be the focus of future studies.

Loss of GSDMD leads to IL-18 hypersecretion during *Shigella flexneri* infection

We next sought to understand the impact of GSDMD on caspase-4-mediated IL-18 production during infection. We generated WT and GSDMD KD human primary intestinal epithelial monolayers (for efficiency of GSDMD KD see Fig. 2a) and infected them with *Shigella flexneri* Δospc3, which induces caspase-4-dependent GSDMD cleavage[38]. Colony forming units (CFUs) recovered from cells after four hours of infection were equivalent between scramble and GSDMD KD cells (Fig. 7a). To monitor plasma membrane pore formation, we imaged PI uptake at 30- minute intervals for the duration of infection. Following 4 h of infection, PI uptake was equivalent between scramble and GSDMD KD cells (Fig. 7b, c) indicating that infection likely induces GSDMD-independent pore formation. Similarly to LPS electroporation, infection resulted in a p37 caspase-4 cleavage fragment in scramble cells but not GSDMD KD cells (Fig. 4d) suggesting that caspase-4 cleavage is induced by GSDMD plasma membrane pore formation and no other membrane pores. The caspase-4 cleavage fragment was detected in the lysate, rather than the supernatant (Fig. 7d) which is likely due to low cell lysis (see Fig. 5e and i). Importantly, loss of GSDMD increased IL-18 production and due to loss of plasma membrane integrity, this was released into the supernatant (Fig. 7e). Together, these data reveal that GSDMD pore formation regulates caspase-4 cleavage into a p37 form and IL-18 production in human intestinal epithelial cells during infection. We believe this represents an important feedback mechanism whereby intestinal epithelial cells can modulate IL-18 production independently of cell death. In conditions of reduced GSDMD plasma membrane pore formation, inhibitory feedback to caspase-4 is limited and IL-18 hyperproduction occurs. This may be an important mechanism to (1) facilitate IL-18 secretion from live cells and (2) amplify cytokine production in the event pyroptosis fails. In summary our data reveals an epithelial-specific role for GSDMD pores in regulating caspase-4 activity and the production of IL-18.

Discussion

Our work demonstrates that GSDMD plasma membrane pores provide a signal to induce caspase-4 cleavage in human epithelial cells and this limits IL-18 production. We propose that this may be a death-independent mechanism to terminate or fine-tune IL-18 production. The significance of this pathway in the epithelium is two-fold. Firstly, by limiting GSDMD plasma membrane pore formation, and prolonging caspase activation, epithelial cells can secrete high levels of IL-18 without compromising barrier integrity. Secondly, while GSDMD-dependent expulsion of epithelial cells is a key defence mechanism against pathogens[7,39], many pathogens have evolved to block pyroptosis[30,40]; thus, in situations where pyroptosis is blocked, and infected cells cannot be ejected from the barrier, increased IL-18 would likely heighten the inflammatory response. This is an effective way to modulate inflammation according to the degree of threat.

A key and unexpected finding was that caspase-4 was active and yet not cleaved when GSDMD plasma membrane pore formation was blocked. Within the inflammasome field, the consensus is that caspase auto-processing is required for catalytic activity against substrates[17,18,41]. However, auto-processing requires induction of catalytic activity, and oligomerization serves as the signal for induction of auto-processing capacity. Thus, it is plausible that oligomerization is sufficient for generation of catalytic activity. Of note, two recent studies characterised the crystal structure of caspase-4 in complex with IL-18[42,43]. Both studies implicated a caspase-4 p20/p10 complex as active against IL-18. It should be noted that in both cases, the p20/p10 complex was ectopically engineered and used as the starting point for crystallization[42] and in ex vivo cleavage assays[43], and thus these studies have not formally shown that this caspase-4 p20/p10 complex naturally occurs in cells following LPS exposure, nor have they excluded that a full-length caspase-4 is active against IL-18. Indeed, our data argue that caspase-4 is active in its full-length form, although it remains possible that ectopic expression of the self-uncleavable form of caspase-4 (D270A/D289A mutant) may cause limited processing of this construct by unknown proteases in this over-expression system. Similarly, a limitation of the caspase-4 over-expression system is that the over-expression itself may trigger activation of unrelated proteases that could impact on IL-18 or GSDMD processing. Future experiments using for instance CRISPR-Cas9-driven knock-in mutations of critical residues within the endogenously expressed caspase-4 should definitely address this point.

In agreement with the notion that caspase-4 is active in its full-length form, there are other reports that caspases are active in their full-length form. Non-cleavable caspase-1 has activity against GSDMD[44], while cleavage generates activity against IL-18. Similarly, full length caspase-8, in a heterodimeric complex with $FLIP_L$ or in a homodimeric complex with itself is sufficient to generate catalytic activity[45]. Moreover, LPS-induced oligomerization of caspase-4 is sufficient to generate activity against the artificial caspase substrate Z-VAD-AMC[46]. Studies reporting caspase-4 cleavage have examined caspase activation in WT cells[18,19,47] and in overexpression systems[48]. We similarly see caspase-4 cleavage under these conditions, and in all cases caspase-4 processing was associated with reduced IL-18 production. We therefore propose that caspase-4 cleavage into the p37 form limits IL-18 processing, and that the caspase-4 cleavage fragment is a by-product of inflammasome activation, rather than the active species. Direct demonstration of this hypothesis will require identifying the protease(s) involved in caspase-4 p37 generation.

It is also interesting to note that the p31 fragment observed in THP1 cells (Fig. 3c, d) and in our HEK overexpression system (Fig. 4i) was not due to caspase-4 autocatalytic activity. Inhibition of NLRP3 prevented p31 generation in THP1 cells and the p31 fragment was observed in HEK cells expressing the catalytically dead caspase-4 mutant C258A. This indicates that other enzymes may cleave caspase-4 and hence alter caspase-4 activity. Interestingly, the cleavage profile observed in HCT116 cells was different to that observed in THP1 cells (Fig. 3a-c). This may indicate different mechanisms of cleavage in a cell-specific manner which may be engaged in a pore-dependent manner to regulate caspase activity.

While we observed that GSDMD pore formation was required for caspase-4 cleavage, we have not determined how the pore relays this signal. Based on caspase dogma, our initial idea was that GSDMD-induced caspase-4 autocatalytic activity led to self-cleavage. However, two pieces of data reshaped our thinking. In Fig. 3d we demonstrate that MCC950 blocks processing of caspase-4 at p31. We also observed that thapsigargin and ER stress induce p37 cleavage without p35 GSDMD cleavage (Supplementary Fig. 2j). Both findings indicate that caspase-4 cleavage is the result of the action of (an)other protease(s), rather than autocatalytic caspase-4 activity. The idea that ER stress induces caspase-4 cleavage is particularly intriguing. The ER is composed of lipid membranes, and it is conceivable that GSDMD pore formation in this organelle causes stress akin to thapsigargin leading to caspase-4 cleavage. Thus far, we have no evidence that GSDMD directly

induces ER stress, and it is possible that GSDMD plasma membrane pore formation and ER stress activate converging pathways that lead to caspase-4 cleavage. Calcium influx controls activation of the ESCRT pathway[13], rearrangement of F-actin[49] and the openness of GSDMD pores[50]. The ER is also a source of intracellular calcium and therefore calcium is an attractive target. However, we observed no effect on IL-18 production by blocking calcium flux with EGTA-AM (Supplementary Fig. 2e-f). Ongoing work is aimed at determining what leads to caspase-4 cleavage.

A key challenge we faced was in distinguishing between the role of cell death and plasma membrane pore formation in limiting IL-18 production. As stated previously, it is likely that dead cells are unable to produce IL-18 and hence that cell death limits IL-18 production to a degree. However, we also believe our data provides evidence that there are mechanisms that regulate cytokine production independently of cell death. If cell death and cytokine production were mutually regulated, any attempt to increase cytokine production would increase GSDMD cleavage and accelerate cell death, thus preventing more cytokine production. To investigate whether cell death was the only factor that regulated IL-18 production, we first considered at what stage following GSDMD cleavage a cell is truly dead. The most widely used measure of pyroptosis are DNA-intercalating viability dies, which measure plasma membrane integrity. The use of these assays has likely shaped how we define a dead cell, as one with plasma membrane pores. As our understanding of pyroptosis evolves, we are becoming aware that pyroptosis is a multi-layered event where death is the result of a cumulation of events including mitochondrial dysfunction[24–26], lysosomal rupture[26] and plasma membrane pore formation[51] and cellular lysis[52]. Our data support the notion that induction of pyroptosis pathway and generation of the GSDMD N-terminal fragment can decrease cellular viability even in the absence of plasma membrane pore formation (Fig. 6a-g, j-l), and that, conversely, cells with plasma membrane GSDMD pores can still be viable (Fig. 6j-l). Considering this, and other works[23–26] that recently codified the impact of GSDMD N-terminal fragment on cellular fitness, including mitochondrial function, we propose that cellular viability during pyroptotic pathway induction is a spectrum. When considering at which point the cell is dead, we propose that different cellular functions can continue to occur during declining cell viability, and there is a sequential dismantling of cellular functions as the cell moves through pyroptosis. This model is more in line with other forms of regulated cell death, including apoptosis and granzyme/perforin mediated cell death. We sought to determine at which point during cell death GSDMD induced caspase-4 cleavage to limit IL-18 production. Our data indicates that GSDMD plasma membrane pore formation induces caspase-4 cleavage (Fig. 6d) and limits IL-18 production (Fig. 6e, i-l). Interestingly, redundant plasma membrane pores did not induce caspase-4 cleavage in the absence of GSDMD (Fig. 7b-d) suggesting specificity of a GSDMD plasma membrane pore – caspase-4 crosstalk signal. Given that it has been proposed that cytokines exit the cell via GSDMD pores, our observations propose the existence of a negative feedback loop in human epithelial cells, whereby GSDMD pores facilitate the release of IL-18 and feedback to inhibit production by inducing cleavage of caspase-4 into a p37 form. A key step is to identify the factor that induces caspase-4 cleavage to determine if inhibiting proteolytic function of this factor during pyroptosis increases IL-18 production. Nevertheless, we believe that our results are an important initial step in understanding how cytokine production is regulated during pyroptosis.

In summary we have identified a mechanism for GSDMD-dependent regulation of the production of IL-18 in the human intestinal epithelium. This mechanism appears to be specific to epithelial cells and may be important in facilitating homoeostatic IL-18 production. We moreover propose that full-length caspase-4 processes IL-18. Our observation that GSDMD regulates inflammasome cytokine production alludes to a previously unidentified pathway through which inflammasome signalling can be modulated to control the balance between cytokine secretion and cell death.

Methods

Cell culture

HCT116, C2bbe1 and HEK293T cells were obtained from ATCC and maintained in Dulbecco's Modified Eagle's Medium (DMEM) (Wisent) supplemented with 10% heat- inactivated foetal bovine serum (FBS; Wisent) and 1% penicillin/streptomycin. THP1 cells obtained from ATCC were maintained in RPMI 1640 media (Wisent) supplemented with 10% heat—inactivated foetal bovine serum (FBS; Wisent) and 0.05 mM 2-mercaptoethanol. Cells were maintained in 95% air, 5% CO_2 and 37 °C. Cells were used for a maximum of 10 passages.

Generation of CRISPR knockout cells

HCT116 knockout cells were generated using the using lentiCRISPRv2 plasmid (Addgene). Guides were designed using Synthego CRISPR design tool and received from IDT. Multiple guides per target were designed. Guides were annealed then cloned into lentiCRISPRv2 plasmid and the resulting plasmid was sequenced. To generate lentivirus, lentiCRISPRv2 plasmid was transfected into HEK293T cells along with pMD2.G and psPAX2 viral envelope and packaging vectors. Virus was harvested 3 days later and used to transduce HCT116 cells. Polyclonal stably expressing cells were selected with puromycin. Monoclonal cultures were generated via the single cell limiting dilution method. Knockouts were screened by western blot and functional assays.

Guides used for Caspase 4 and GSDMD are provided in Supplementary Table 1.

Generation of shRNA stable knockdown cells

shRNA knockdowns were generated using the pLKO.1 expression vector. shRNA constructs were designed and received from IDT. shRNA constructs were annealed then cloned into pLKO.1 expression vector. The vector was sequenced. Lentivirus was generated by transfecting HEK293T cells with shRNA, pMD2.G and psPAX2 viral envelope and packaging vectors. Virus was harvested three days later. Transduced cells were selected by addition of the selection marker puromycin to culture three days after viral transduction. Human organoid stable knockdowns were generated following protocols optimized by Miyoshi et al.[53]. Knockdown of targeted protein was validated by western blot, functional assays or qPCR as indicated.

shRNA constructs used are provided in Supplementary Table 1.

siRNA knockdown of cells

To generate transient knockdown of targets, Silencer select siRNA (ambion life technologies) was transfected into cells using Lipofectamine RNAi MAX transfection reagent. Knockdown of target protein was validated by western blot or qPCR. Cells were used for experiments three days following transfection.

siRNA used are provided in Supplementary Table 1.

Electroporation of cells

To activate inflammasomes, cells were harvested and resuspended in 100µL of Ingenio® EZporator® Electroporation Solution (Mirus Bio). Ligand was added (2µg LPS for epithelial cells, 1 µg LPS for THP1 cells) and cells were nucleofected using the Amaxa Nucleofector® 1 device. Cells were placed into fresh culture medium and left for 3 h.

Cell cytotoxicity assay (LDH release)

Cell supernatant was harvested by centrifugation at 400 x *g*. 25 µL of supernatant was diluted in 75 µL of water. Percentage cell death was measured using Cell Cytotoxicity Detection kit (LDH; Sigma) as per manufacturer's instructions.

Cell viability assay (ATP production)

Cell viability assays were conducted as per the protocol for Promega CellTitre-GLO® 2.0 Cell Viability Assay. Briefly, following stimulation, 100 µL of cells and supernatant were collected into black well clear bottom 96 well plates. Assay reagent was added, cells were placed on shaker for 2 min then

luminescence was read on a SpectraMax® i3 Spectrophotometer (Molecular Devices).

Propidium Iodide uptake

Following addition of gentamycin (organoid monolayers) or following transfection (HEK293T cells), 1 µg/mL propidium iodide was added to cell culture media. Cells were placed into an Incucyte® Live-Cell Analysis System (Sartorius). Images were taken every half hour (for *Shigella* infection) or every hour for HEK293T cells. For *Shigella* infections, PI positivity was calculated by normalising the number of red objects per area of confluent cells. For HEK293T assays, PI uptake was calculated by comparing mean fluorescence intensity (MFI) of GSDMD- transfected HEKs to mock transfected HEKs.

Western blotting

Cells were harvested in Radioimmunoprecipitation Assay Buffer (RIPA). Protein was quantified using BCA protein assay kit (Thermo). Samples were normalised in RIPA buffer and SDS-PAGE denaturing sample buffer. SDS-PAGE was conducted using standard techniques. Gels were transferred on to polyvinylidene fluoride membrane using a semi- dry transfer apparatus and blocked using 2.5% BSA. Primary antibodies were diluted at indicated concentrations and incubated overnight at 4 °C. Blots were washed 3x in 0.1% TBS-T. Secondary antibodies were diluted at a concentration of 1:10000 in 2.5% BSA in 0.1%TBS-T and incubated for 1 h at room temperature. Blots were washed 4x then developed using SuperSignal™ West Femto Maximum Sensitivity Substrate (Thermo), or Luminata Classico Western HRP substrate (Fisher Scientific). Molecular weight markers that were ran alongside with samples were not exported with the original acquisitions on our Chemidoc instrument, but were added post hoc by aligning blots to the physical membranes.

ELISA

For analysis of secreted IL-18 supernatants of electroporated cells were collected and spun at 400 x *g* to remove cells. For measurement of total IL-18, cells and supernatant were collected and, 10µL of 33% Triton-X in PBS was added per 1 mL supernatant to lyse cells into supernatant. Supernatants and lysed cell suspensions were pelleted at 10,000 x *g* to remove cell debris. IL-18 was measured using Human Total IL-18 DuoSet ELISA (R&D Systems) as per manufacturer's instructions.

qPCR

Cell pellets were washed in PBS. Total RNA was isolated using GeneJET RNA purification kit (Thermo Fisher). Genomic DNA was lysed using amplification grade DNase 1 (Invivogen) as per manufacturer's instructions. 800 ng-1 µg of RNA was reverse transcribed in a mix containing M-MLV reverse transcriptase (Invivogen), dNTP mix (Biobasic), RNaseOUT™ Recombinant Ribonuclease Inhibitor (Thermo Fisher), Random Hexamer Primers (Thermo Fisher), oligoDT(18) primers (Thermo Fisher). cDNA was amplified using primers from IDT and PowerUp SYBR Green master mix (Thermo Fisher) as per manufactures instructions.

Primers for qPCR are provided in Supplementary Table 1.

Plasmid generation and overexpression

pcDNA3.1 vectors expressing human caspase-4, human IL-18 and human GSDMD were purchased from Genscript. GSDMD Mutagenesis primers were designed using Aligent Quik change primer design. Mutagenesis was conducted using QuikChangeII site directed mutagenesis kit as per manufactures instructions and mutations were validated by sequencing. Mutagenesis primers are provided in Supplementary Table 1.

Transient transfections

1 µg of each plasmid or pcDNA3.1 empty vector was reverse transfected into 1×10^6 HEK293T cells using FUGENE HD (Promega) as per manufactures instructions. Cells were harvested 16 h post transfection.

Organoid generation and culture

0.5 cm pinch biopsies were harvested from fresh human duodenal tissue. Tissue was minced until able to be passed through a 1 mL pipette tip then incubated in 2 mg/mL collagenase at 37 °C for 40 min. Crypt units were dissociated by vigorous pipetting then washed 3x in PBS containing 10% FBS and plated into 40 µL Matrigel domes (Cultrex PathClear reduced growth factor BME, type 2; R&D Systems) in a 24 well plate. Cultures were maintained in media following procedures optimized by Bugda Gwilt et al.[54]. For monolayer generation, organoids were disrupted into single cells then seeded at a density of 5×10^5 in a 24 well plate precoated with 1:40 matrigel. Monolayers were left to grow for 3 days before infection.

Shigella flexneri infections

Shigella strains were a generous gift from Dr John Rhode (Dalhousie University, Canada). *Shigella flexneri* was sub-cultured in Trypsin Soy Broth (TSB) broth containing 100 µg/mL of appropriate antibiotic for approximately 2.5 h until culture reached an OD600 = 0.45 *Shigella* cultures were washed 1x in PBS then added to cells at MOI = 100. Cells were centrifuged for 10 min at 500 x *g* then returned to the incubator for 45 min. Following this, cells were washed 3x in PBS then media containing gentamycin (Gibco) at a final concentration of 50 µg/mL was added to kill extracellular bacteria. Cells were harvested 4 h post infection.

Organoid inflammasome stimulation

On day 6 following passaging, organoids were removed from Matrigel and broken into smaller cell clusters with TrypLE Express (Gibco). After 1 wash, cells were electroporated using Mouse/Rat Hepatocyte NucleofectorTM Kit (Lonza) and Amaxa Nucleofector® 1 device and LPS (2 µg). Following electroporation, cells were pelleted to remove electroporation solution and then resuspended in in 200µL of fresh media for 2 h.

Antibodies and other reagents

Unless indicated, all antibodies were used at 1/500 dilution from the concentrations provided by the supplier. Rabbit anti-GSDMD (HPA044487; Sigma), mouse anti-Caspase-4 (M029-3, Marine BL), rabbit anti-caspase-1 (3866S; Cell Signalling Technology), rabbit anti-Caspase-5 (ab40887; abcam), goat anti- IL-18 (AF2548; Novus Biologicals), anti-Tubulin (T9026, Millipore Sigma, 1/10,000 dilution), LPS (14011S; CST), human IFNγ (80385S; Cell Signalling Technology), Nigericin (N7143; Sigma), Z-VAD-FMK (tlrl-vad; InvivoGen), VX-765 (7143/50, Cedarlane), peroxidase conjugated anti-rabbit and anti-mouse secondaries (Jackson Labs, 111-035-003), peroxidase conjugated anti-goat secondary (HAF109; R&D Systems).

Statistics and reproducibility

Prism software was used to plot data and determine statistical significance using analysis of variance (ANOVA) with multiple comparisons Data are presented as S.E.M as indicated. A p value of 0.05 or less was considered statistically significant. For all experiments, measurements were taken from distinct biological samples and not technical replicates. Moreover, all the data presented are representative of at least $N = 3$ biological replicates, unless specifically indicated.

Statement of Ethics

Human samples were collected under protocols approved by the University of Toronto Research Ethics Board (UofT REB no. 27930). Informed consent was obtained from all donors prior to obtaining tissue. All ethical regulations relevant to human research participants were followed.

Data availability

Data are available from the corresponding author on reasonable request. Uncropped blots and gels for all the experiments presented in the manuscript can be found in Supplementary Fig. 3. Source data can be found in Supplementary Data 1.

Received: 21 August 2023; Accepted: 6 May 2025;
Published online: 13 May 2025

References

1. Winsor, N., Krustev, C., Bruce, J., Philpott, D. J. & Girardin, S. E. Canonical and noncanonical inflammasomes in intestinal epithelial cells. *Cell Microbiol* **21**, e13079 (2019).
2. Sborgi, L. et al. GSDMD membrane pore formation constitutes the mechanism of pyroptotic cell death. *EMBO J.* **35**, 1766–1778 (2016).
3. Shi, J. et al. Cleavage of GSDMD by inflammatory caspases determines pyroptotic cell death. *Nature* **526**, 660–665 (2015).
4. Evavold, C. L. et al. The pore-forming protein gasdermin D regulates interleukin-1 secretion from living macrophages. *Immunity* **48**, 35–44.e36 (2018).
5. Chen, X. et al. Pyroptosis is driven by non-selective gasdermin-D pore and its morphology is different from MLKL channel-mediated necroptosis. *Cell Res.* **26**, 1007–1020 (2016).
6. Jorgensen, I., Zhang, Y., Krantz, B. A. & Miao, E. A. Pyroptosis triggers pore-induced intracellular traps (PITs) that capture bacteria and lead to their clearance by efferocytosis. *J. Exp. Med.* **213**, 2113–2128 (2016).
7. Rauch, I. et al. NAIP-NLRC4 inflammasomes coordinate intestinal epithelial cell expulsion with eicosanoid and IL-18 release via activation of caspase-1 and -8. *Immunity* **46**, 649–659 (2017).
8. Samperio Ventayol, P. et al. Bacterial detection by NAIP/NLRC4 elicits prompt contractions of intestinal epithelial cell layers. *Proc. Natl. Acad. Sci. USA* **118**, e2013963118 (2021).
9. Holly, M. ayumi et al. Salmonella enterica Infection of Murine and Human Enteroid-Derived Monolayers Elicits Differential Activation of Epithelium-Intrinsic Inflammasomes. *Infect. Immun.* **88**, e00017–e00020 (2020).
10. Knodler, L. A. et al. Noncanonical inflammasome activation of caspase-4/caspase-11 mediates epithelial defenses against enteric bacterial pathogens. *Cell Host microbe* **16**, 249–256 (2014).
11. Chiang, H.-Y. et al. IL-22 initiates an IL-18-dependent epithelial response circuit to enforce intestinal host defence. *Nat. Commun.* **13**, 874 (2022).
12. Müller, A. A. et al. An NK cell perforin response elicited via IL-18 controls mucosal inflammation kinetics during salmonella gut infection. *PLOS Pathog.* **12**, e1005723 (2016).
13. Rühl, S. et al. ESCRT-dependent membrane repair negatively regulates pyroptosis downstream of GSDMD activation. *Science* **362**, 956–960 (2018).
14. Zhivaki, D. et al. Inflammasomes within hyperactive murine dendritic cells stimulate long-lived T cell-mediated anti-tumor immunity. *Cell Rep.* **33**, 108381 (2020).
15. Zanoni, I. et al. An endogenous caspase-11 ligand elicits interleukin-1 release from living dendritic cells. *Science* **352**, 1232–1236 (2016).
16. Rühl, S. & Broz, P. Regulation of lytic and non-lytic functions of gasdermin pores. *J. Mol. Biol.* **434**, 167246 (2022).
17. Boucher, D. et al. Caspase-1 self-cleavage is an intrinsic mechanism to terminate inflammasome activity. *J. Exp. Med.* **215**, 827–840 (2018).
18. Wang, K. et al. Structural mechanism for GSDMD targeting by autoprocessed caspases in pyroptosis. *Cell* **180**, 941–955.e920 (2020).
19. Wandel, M. P. et al. Guanylate-binding proteins convert cytosolic bacteria into caspase-4 signaling platforms. *Nat. Immunol.* **21**, 880–891 (2020).
20. Woods, W. et al. VX-765, an orally available selective interleukin converting enzyme (ICE)/caspase-1 inhibitor exhibits potent anti-inflammatory activities by inhibiting the release of IL-1b and IL-18. *J. Pharmacol. Exp. Ther.* https://doi.org/10.1124/jpet.106.111344 (2007).
21. Borges, J. P. et al. Glycine inhibits NINJ1 membrane clustering to suppress plasma membrane rupture in cell death. *eLife* **11**, e78609 (2022).
22. Humphries, F. et al. Succination inactivates gasdermin D and blocks pyroptosis. *Science* **369**, 1633–1637 (2020).
23. Balasubramanian, A. et al. The palmitoylation of gasdermin D directs its membrane translocation and pore formation during pyroptosis. *Sci. Immunol.* **9**, eadn1452 (2024).
24. Du, G. et al. ROS-dependent S-palmitoylation activates cleaved and intact gasdermin D. *Nature* https://doi.org/10.1038/s41586-024-07373-5 (2024).
25. Miao, R. et al. Gasdermin D permeabilization of mitochondrial inner and outer membranes accelerates and enhances pyroptosis. *Immunity* **56**, 2523–2541.e2528 (2023).
26. de Vasconcelos, N. M., Van Opdenbosch, N., Van Gorp, H., Parthoens, E. & Lamkanfi, M. Single-cell analysis of pyroptosis dynamics reveals conserved GSDMD-mediated subcellular events that precede plasma membrane rupture. *Cell Death Differ.* **26**, 146–161 (2019).
27. Xia, S. et al. Gasdermin D pore structure reveals preferential release of mature interleukin-1. *Nature* **593**, 607–611 (2021).
28. Ding, J. et al. Pore-forming activity and structural autoinhibition of the gasdermin family. *Nature* **535**, 111–116 (2016).
29. Kuang, S. et al. Structure insight of GSDMD reveals the basis of GSDMD autoinhibition in cell pyroptosis. *Proc. Natl. Acad. Sci. USA* **114**, 10642–10647 (2017).
30. Chai, Q. et al. A bacterial phospholipid phosphatase inhibits host pyroptosis by hijacking ubiquitin. *Science* **378**, eabq0132 (2022).
31. Xu, J. et al. Constitutively active autophagy in macrophages dampens inflammation through metabolic and post-transcriptional regulation of cytokine production. *Cell Rep.* **42**, 112708 (2023).
32. Branco, L. M. et al. Lysosomal cathepsins act in concert with Gasdermin-D during NAIP/NLRC4-dependent IL-1β secretion. *Cell Death Dis.* **13**, 1029 (2022).
33. Chevriaux, A. et al. Cathepsin B is required for NLRP3 inflammasome activation in macrophages, through NLRP3 interaction. *Front Cell Dev. Biol.* **8**, 167 (2020).
34. van de Veerdonk, F. L. et al. Reactive oxygen species-independent activation of the IL-1beta inflammasome in cells from patients with chronic granulomatous disease. *Proc. Natl. Acad. Sci. USA* **107**, 3030–3033 (2010).
35. Vijayaraj, S. L. et al. The ubiquitylation of IL-1β limits its cleavage by caspase-1 and targets it for proteasomal degradation. *Nat. Commun.* **12**, 2713 (2021).
36. Hitomi, J. et al. Involvement of caspase-4 in endoplasmic reticulum stress-induced apoptosis and Aβ-induced cell death. *J. Cell Biol.* **165**, 347–356 (2004).
37. Tsuru, A., Imai, Y., Saito, M. & Kohno, K. Novel mechanism of enhancing IRE1α-XBP1 signalling via the PERK-ATF4 pathway. *Sci. Rep.* **6**, 24217 (2016).
38. Li, Z. et al. Shigella evades pyroptosis by arginine ADP-riboxanation of caspase-11. *Nature* **599**, 290–295 (2021).
39. Mitchell, P. S. et al. NAIP–NLRC4-deficient mice are susceptible to shigellosis. *eLife* **9**, e59022 (2020).
40. Luchetti, G. et al. Shigella ubiquitin ligase IpaH7.8 targets gasdermin D for degradation to prevent pyroptosis and enable infection. *Cell Host Microbe* **29**, 1521–1530.e1510 (2021).
41. Julien, O. & Wells, J. A. Caspases and their substrates. *Cell Death Differ.* **24**, 1380–1389 (2017).
42. Devant, P. et al. Structural insights into cytokine cleavage by inflammatory caspase-4. *Nature* **624**, 451–459 (2023).
43. Shi, X. et al. Recognition and maturation of IL-18 by caspase-4 noncanonical inflammasome. *Nature* **624**, 442–450 (2023).
44. Broz, P., von Moltke, J., Jones, J. W., Vance, R. E. & Monack, D. M. Differential requirement for caspase-1 autoproteolysis in pathogen-

induced cell death and cytokine processing. *Cell Host Microbe* **8**, 471–483 (2010).
45. Pop, C. et al. FLIP(L) induces caspase 8 activity in the absence of interdomain caspase 8 cleavage and alters substrate specificity. *Biochem. J.* **433**, 447–457 (2011).
46. Shi, J. et al. Inflammatory caspases are innate immune receptors for intracellular LPS. *Nature* **514**, 187–192 (2014).
47. Casson, C. N. et al. Human caspase-4 mediates noncanonical inflammasome activation against gram-negative bacterial pathogens. *Proc. Natl. Acad. Sci.* **112**, 6688–6693 (2015).
48. Amy, H. C. et al. Caspase-4 dimerisation and D289 auto-processing elicit an interleukin-1β-converting enzyme. *Life Sci. Alliance* **6**, e202301908 (2023).
49. Zhang, J. et al. Epithelial Gasdermin D shapes the host-microbial interface by driving mucus layer formation. *Sci. Immunol.* **7**, eabk2092 (2022).
50. Santa Cruz Garcia, A. B., Schnur, K. P., Malik, A. B. & Mo, G. C. H. Gasdermin D pores are dynamically regulated by local phosphoinositide circuitry. *Nat. Commun.* **13**, 52 (2022).
51. Devant, P. et al. Gasdermin D pore-forming activity is redox-sensitive. *Cell Rep.* **42**, 112008 (2023).
52. Kayagaki, N. et al. NINJ1 mediates plasma membrane rupture during lytic cell death. *Nature* **591**, 131–136 (2021).
53. Miyoshi, H. & Stappenbeck, T. S. In vitro expansion and genetic modification of gastrointestinal stem cells in spheroid culture. *Nat. Protoc.* **8**, 2471–2482 (2013).
54. Gwilt, K. B. & Thiagarajah, J. R. Strategies for optimizing the isolation and expansion of sensitive patient-derived duodenoids, ileoids and colonoids. *protocols.io* https://content.protocols.io/files/mgzvbdqn7.pdf (2023).

Acknowledgements

This work was supported by grants from the Canadian Institutes of Health Research (CIHR) and the Crohn's Colitis Canada (CCC) to SEG and DJP.

Author contributions

S.E.G., J.K.B., D.J.P., J.E.L., J.R.R. and S.K. designed the experiments. L.Y.L. and Y.T. performed THP1 experiments, E.G.F., N.J.W. and P.Y.B. performed experiments critical to shaping ideas in the paper. C.K. created CRISPR knockout cells. H.Y.G provided human tissue samples. J.K.B. performed all other experiments and analyses.

Competing interests

The authors declare no competing interests.

Additional information

Supplementary information The online version contains supplementary material available at https://doi.org/10.1038/s42003-025-08183-9.

Correspondence and requests for materials should be addressed to S. E. Girardin.

Peer review information *Communications Biology* thanks Jixi Li and the other, anonymous, reviewer(s) for their contribution to the peer review of this work. Primary Handling Editors: Liming Sun and David Favero. A peer review file is available.